Development of Thermoelectric Materials with Improved Figure of Merit for Better Conversion Efficiency

Helmut Baumgart [1,2]

[1] Department of Electrical and Computer Engineering
Old Dominion University, Norfolk, Virginia 23529, USA

[2] Applied Research Center at Thomas Jefferson National Accelerator Laboratories
Newport News, Virginia 23606, USA

5th International Workshop on Low Temperature Bonding for 3D Integration
LTB-3D 2017
May 16-18, 2017
The University of Tokyo, Tokyo, Japan

Outline

- Introduction to Thermoelectric Principles vs. Photovoltaics
- Methods to Enhance Thermoelectric Conversion Efficiency
- Experiments
  - Thermoelectric nanolaminate Films of ALD Bi_2Te_3/Sb_2Se_3
  - Case study ALD Synthesis of PbTe/ PbSe thermoelectric Nanolaminates
  - Use of Porous Templates & Nanostructuring to improve Figure of Merit
  - Seebeck Measurements of structured ALD thermoelectric Nanolaminates
- Results and Discussions
- Conclusions

Photovoltaics: Green Renewable Energy from Absorbed Sunlight

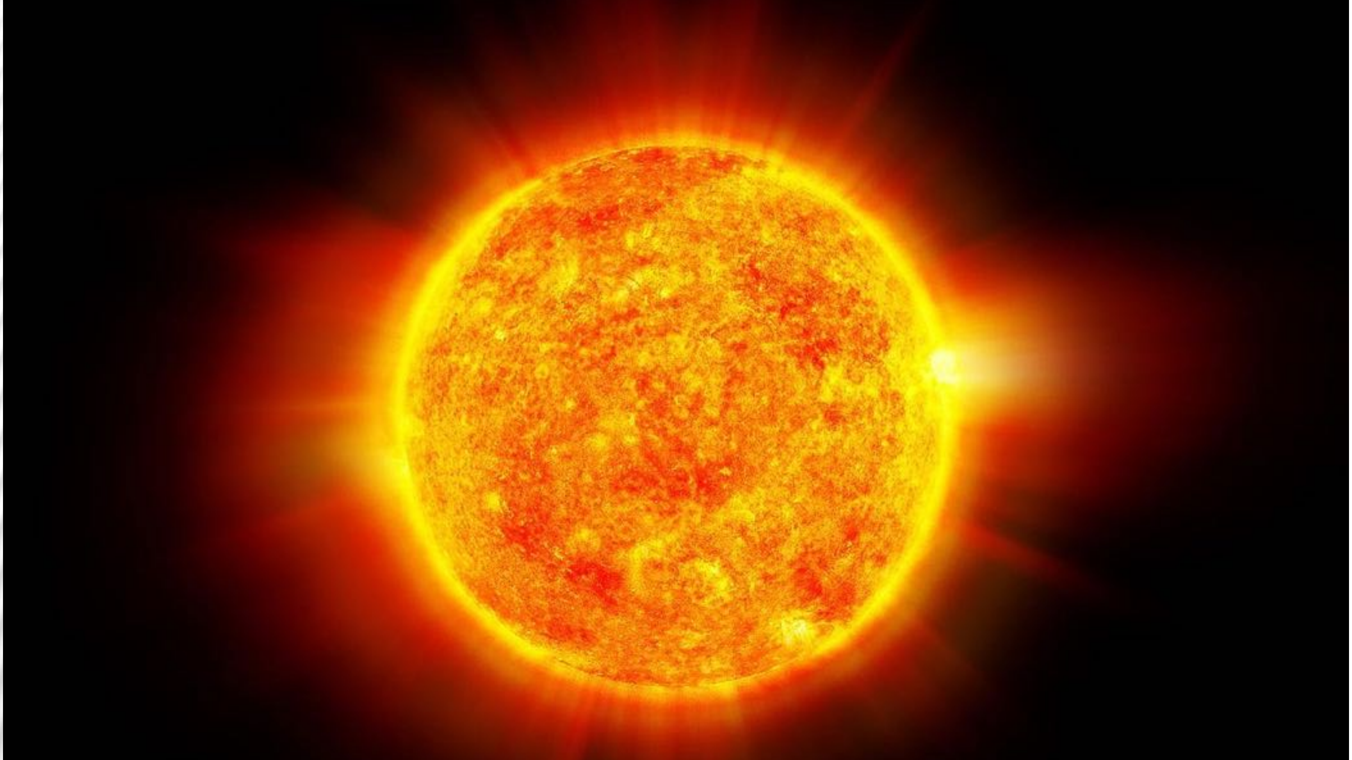

The Energy that all humans use in one year is equivalent to $\Rightarrow$ **one hour** of sunlight striking the earth.

OPERATION OF SOLAR CELLS

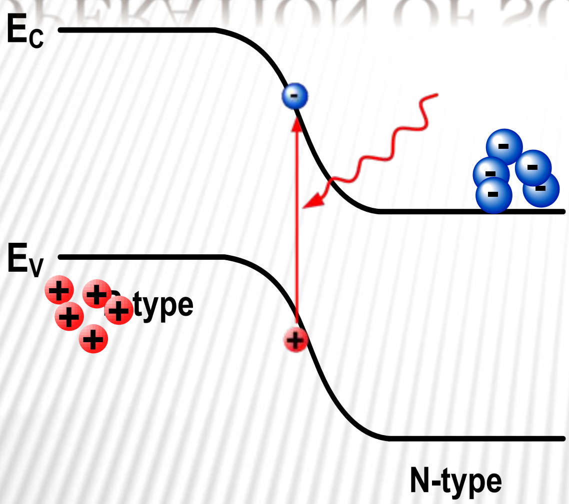

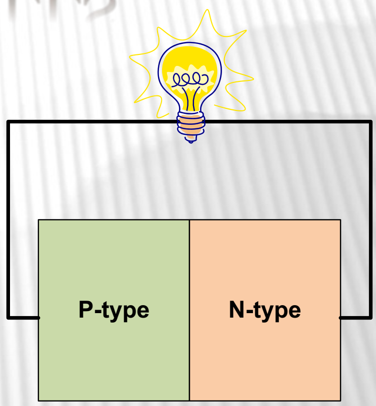

Create current, called short circuit current : $\mathbf{J_{SC}}$

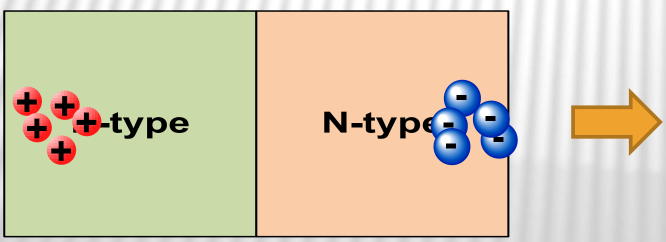

Create voltage, called open circuit voltage V_{OC}

OPERATION OF SOLAR CELLS

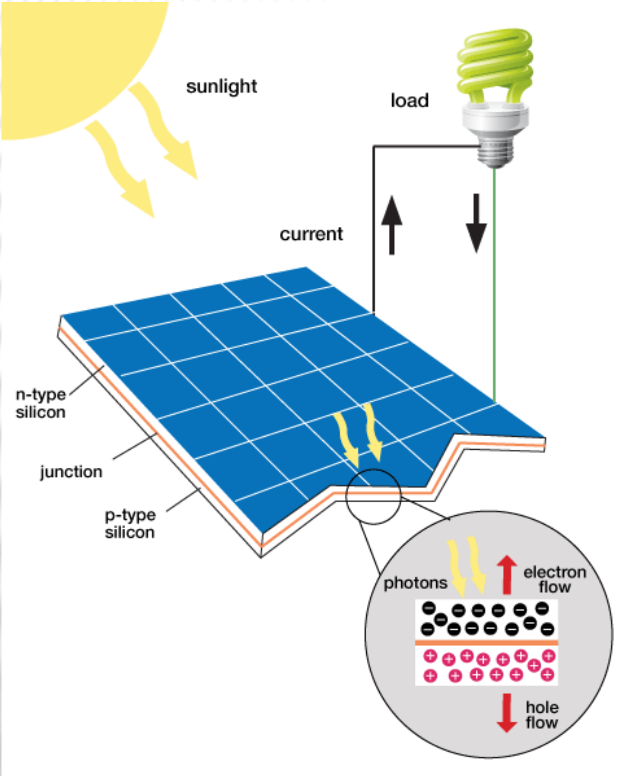

Thermoelectrics: Waste Heat Recovery to Generate Electricity – Green renewable Energy

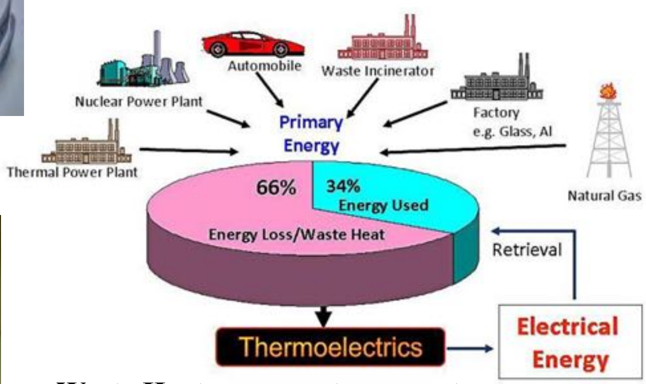

Waste Heat recovery to generate green energy

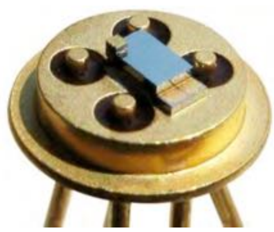

TE cooler: Telecoms laser

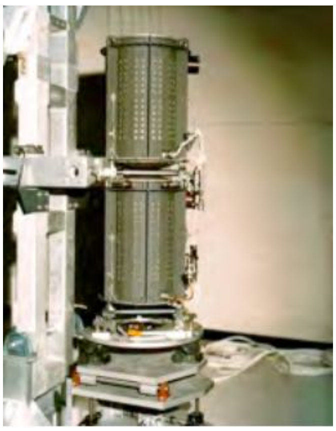

NASA Voyager I & II

Photovoltaics & Thermoelectrics

constitute green renewable energy !!

Microprocessor cooler

▪ The Principal Thermoelectric Effects

1. Seebeck Effect

An electrical potential (voltage) within a junction of two dissimilar conductors is generated due to a temperature gradient.

$$V = \int_{T_1}^{T_2} S_{AB}\, dT \qquad S = -\frac{\Delta V}{\Delta T}$$

2. Peltier Effect

Heat is absorbed or released at the junction of two dissimilar conductors when a current flows across the interface.

$$Q = \Pi_{AB}\, I$$

3. Thomson Effect

Heat is absorbed or released along a single homogeneous current-carrying conductor with a temperature gradient.

$$Q = \beta I \Delta T$$

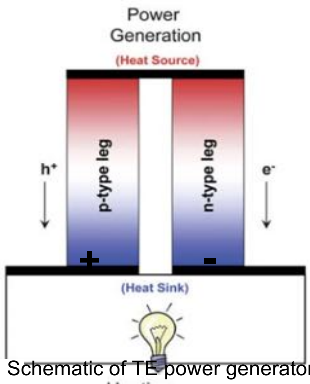

Schematic of TE power generator*

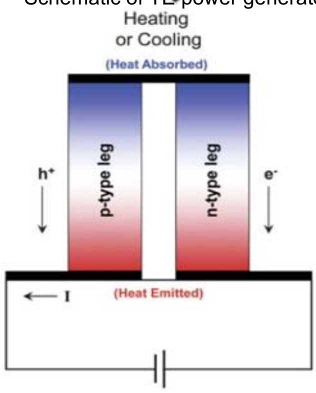

Schematic of TE refrigerator*

Rowe, David Michael, ed. *CRC handbook of thermoelectrics*. CRC press, 1995.

*Szczech, Jeannine R., Jeremy M. Higgins, and Song Jin. *Journal of Materials Chemistry* 21.12 (2011): 4037-4055.

Introduction to Thermoelectrics

The challenge for Thermoelectrics is to increase efficiency.

▪ Efficiency of Thermoelectric (TE) Materials

The efficiency of TE power generators and TE refrigerators is expressed by ε and η:

$$\varepsilon = \frac{T_H - T_C}{T_H}\left[\frac{(1+ZT)^{1/2}-1}{(1+ZT)^{1/2}+(T_C/T_H)}\right] \text{ (TE power generator)}$$

$$\eta = \frac{T_C[(1+ZT)^{1/2}-T_H/T_C]}{(T_H-T_C)[(1+ZT)^{1/2}+1]} \text{ (TE refrigerator)}$$

Where T_C, T_H are cold-side, hot-side temperature, respectively. ZT is the figure of merit.

Chen, Zhi-Gang, et al. *Progress in Natural Science: Materials International* 22.6 (2012): 535-549.

Concept of Thermoelectric Generators

1. Strategy to improve Figure of Merit ZT

The efficiency of a thermoelectric material is determined by the dimensionless thermoelectric figure of merit,

$$ZT = \frac{S^2 \sigma T}{\kappa_e + \kappa_L}$$

where S is the Seebeck coefficient, σ is the electrical conductivity, and ϰ is the thermal conductivity. Seebeck coefficient also known as Thermopower. The thermal conductivity actually is consisting from electron and phonon contributions

$$\kappa = \kappa_e + \kappa_p$$

To improve upon the *ZT*, the Seebeck coefficient and electrical conductivity must increase, whereas the thermal conductivity ϰ must decrease.

❑The ZT of the material is related to the efficiency η of the Thermoelectric device,

$$\eta = \gamma \frac{(1+ZT)^{1/2} - 1}{(1+ZT)^{1/2} + T_{hot}/T_{cold}}$$

where γ is the Carnot efficiency and T_{hot} and T_{cold} are temperatures (in K) of the hot and cold side of the Thermoelectric material.

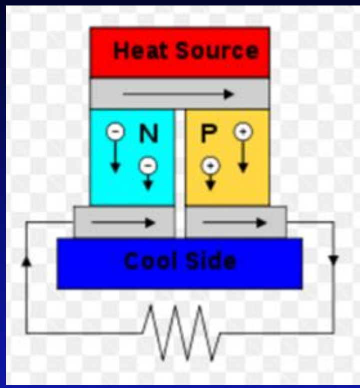

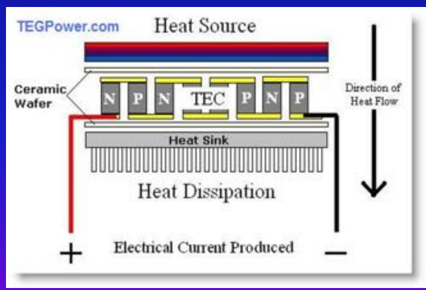

Schematics of principle of thermoelectric generators

Addressed Problem

Thermoelectric energy conversion holds large promise in applications spanning from improved efficiency car engines to energy sources of satellites, to converting industrial waste heat etc. However, the conversion efficiency of thermoelectric devices is sizably lower than practically needed. low efficiency (currently much less than 10%).

$$ZT = \frac{S^2 \sigma T}{\kappa_e + \kappa_L}$$

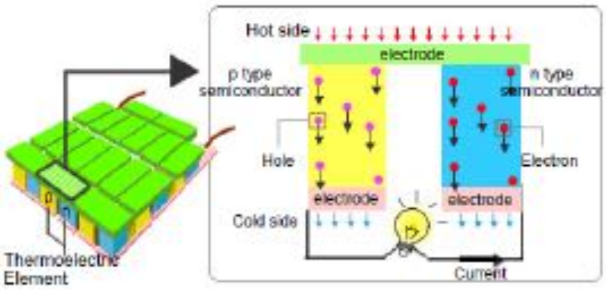

- **Engineering Strategies to Improve the thermoelectric Figure of Merit**

- **(1) ZT is maximized when the average electron energy deviates from the Fermi energy**
- **(2) To optimize σ, increase the number of free carriers**
- **(3) To minimize k, increase phonon scattering => decrease thermal conductivity**
- **(4) to further decrease thermal conductivity utilize porous templates**
- **(5) We propose Nanostructuring & Porous Templates for Phonon Engineering**

▪ Efficiency of Thermoelectric (TE) Material

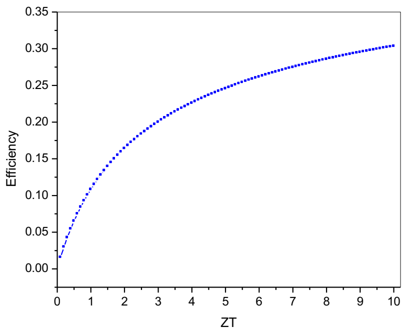

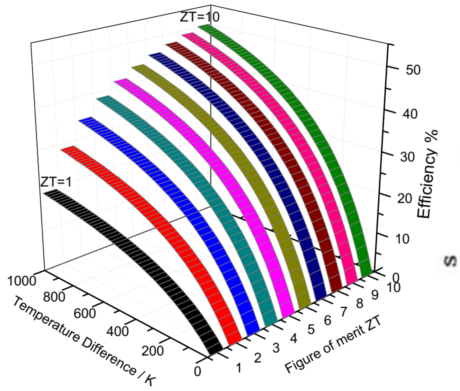

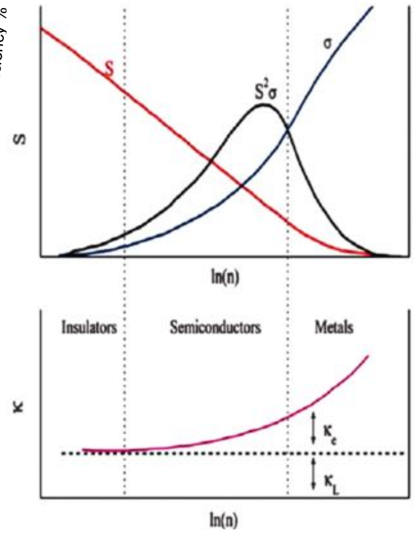

Illustration of the variation of the Seebeck coefficient **S,** electrical conductivity σ ,and thermal conductivity **k** as a function of the charge carrier concentration n for bulk material.

C. Wood, Materials for thermoelectric energy conversion, Reports on Progress in Physics 51(1988)

- The conversion efficiency of TE materials is related to a quantity, figure of merit ZT, which is defined as:

$$ZT = \frac{S^2 \sigma T}{\kappa_e + \kappa_L}$$

Where

S: Seebeck coefficient

σ: Electrical conductivity

T：Temperature

κ_e: Thermal conductivity due to electrons

κ_L : Thermal conductivity due to phonons or lattice vibrations

Frank Batten College of
Engineering & Technology
Old Dominion University: www.eng.odu.edu

Applied Research Center
Old Dominion University

Methods to Enhance Thermoelectric Conversion Efficiency

✓ Phonon glass electron crystal

Glass-like thermal conductivity
Crystal-like electronic properties

✓ Nanostructured TE materials

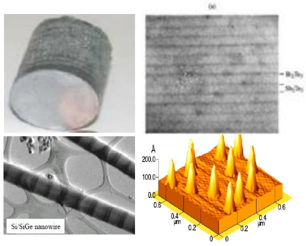

(a) bulk material, (b) 2-D structure,
(c) 1-D structure, (d) 0-D structure

$$ZT = \frac{\boxed{S^2 \sigma} T}{\kappa_e + \kappa_L}$$

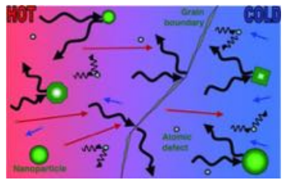

Phonon Scattering Mechanism and
Electrons Transport within TE Materials

Mid / long wavelength phonon
Short wavelength phonon
Hot electrons
Cold electrons

Chen, Zhi-Gang, et al. *Progress in Natural Science: Materials International* 22.6 (2012): 535- 549.

✓ Phononic crystal (PnC) nanostructure

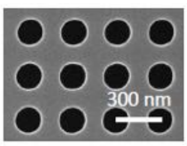

2D PnC, square lattice
period =300 nm

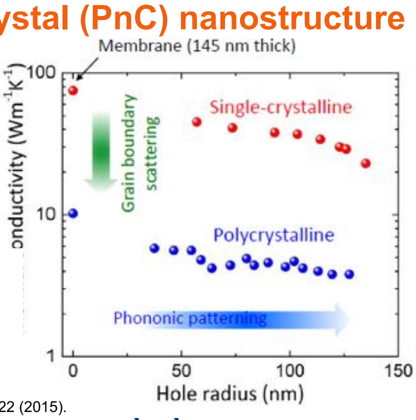

Physical Review B **91**, 205422 (2015).

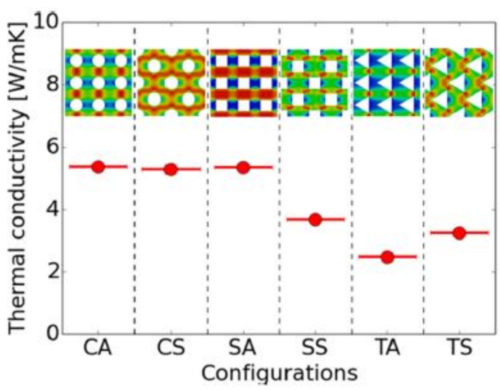

Phonon thermal conductivity for different configurations.
Appl. Phys. Lett. **105**,033116 (2014).

Old Dominion University: www.eng.odu.edu

Applied Research Center
Old Dominion University

▪ State-of-the-art Figures of Merit ZT for Various Classes Thermoelectric Materials

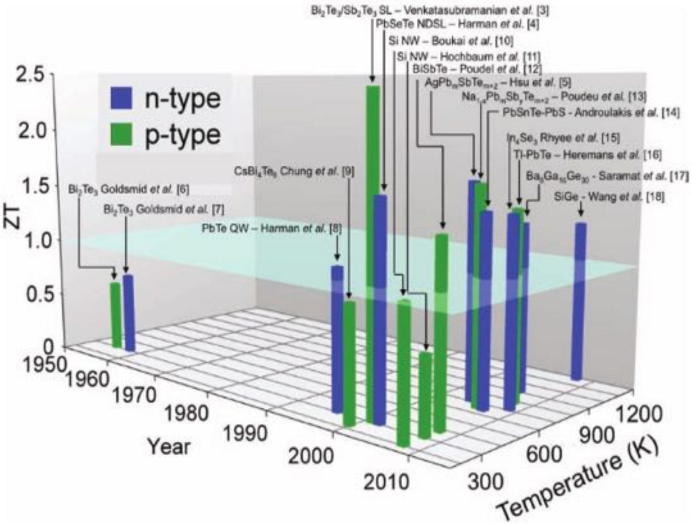

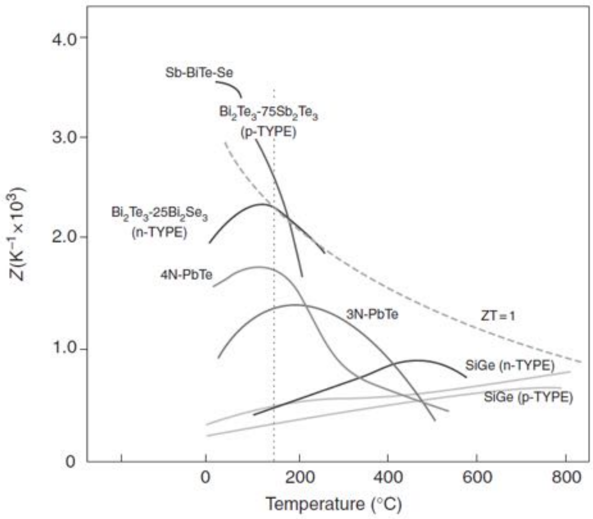

Source: Thermoelectrics handbook :Macro to nano Edited by D.M.Rowe

Major milestones achieved for ZT as a function of both year and temperature

❖ Different TE materials work only for specific temperature application range.

Vineis, Christopher J., et al. "Nanostructured thermoelectrics: big efficiency gains from small features." *Advanced Materials* 22.36 (2010): 3970-3980.

▪ Methods to Enhance Thermoelectric Conversion Efficiency

✓ Nanostructured TE materials

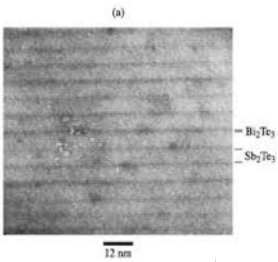

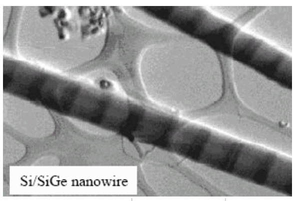

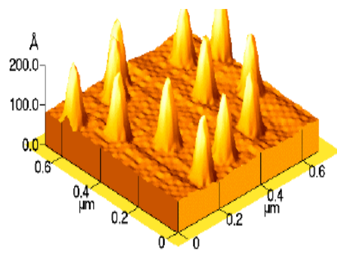

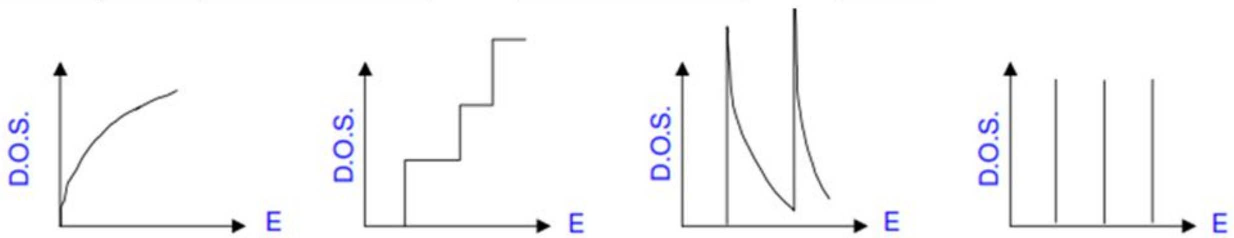

Schematic illustration of density of states as a function of energy for (a) bulk material, (b) 2-D structure, (c) 1-D structure, (d) 0-D structure

Guan, Yonghui, and Jingying Xie. "Recent developments in low-dimensional thermoelectric materials."

▪ Methods to Enhance Thermoelectric Conversion Efficiency

✓ Concept of Phonon Engineering and utilization of Nano-patterning in order to Decrease Thermal conductivity

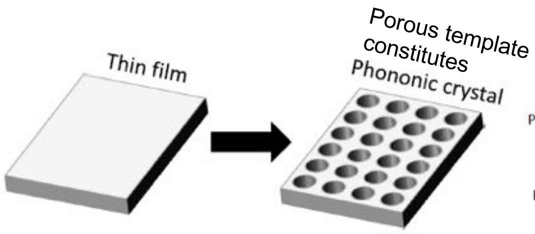

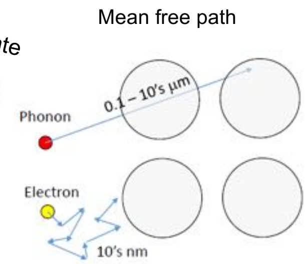

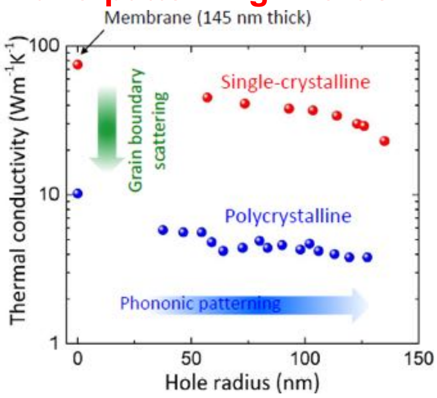

Physical Review B **91**, 205422 (2015).

Proper dimension choice:

- Block phonons
- Not hindering electrons

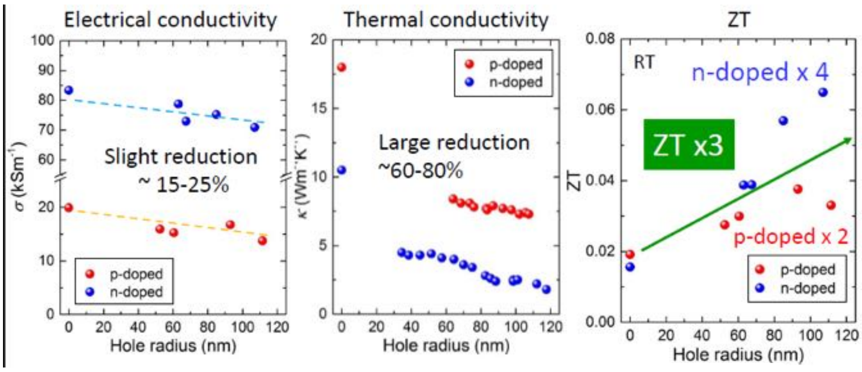

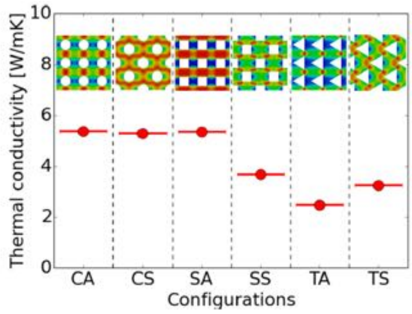

Phonon thermal conductivity for different configurations. APL. **105**,033116 (2014).

3× ZT enhancement by nano-patterning

M. Nomura et al., APL 106, 223106 (2015)

▪ Methods to Enhance Thermoelectric Conversion Efficiency

✓ Nanostructuring of Thermoelectric materials

$$ZT = \frac{S^2 \sigma T}{\kappa_e + \kappa_L}$$

Table.Typical examples of thermal conductivity k & ZT for Nanostructured Thermoelectric materials

Dimension	Structure	Materials	K (Wm^{-1}K^{-1})	ZT
2-D	Quantum Wells, Superlattices	Bi_2Te_3/Sb_2Te_3 [1]	0.22	2.4
		$PbTe/PbTe_{0.75}Se_{0.25}$ [2]	0.5	1.75 (425 K)
1-D	Nanowires	InSb [3], Bi-based [4] , Silicon Nanowire [5]	0.76 (Si)	1 (Si)
0-D	Quantum Dots	PbTe/PbSe QDSLs [6]	0.33	1.6 (300 K)
		$AgPb_mSbTe_{2-m}$ [7] (LAST-18)	0.5~0.8	1.7 (700 K)
		$NaPb_mSbTe_{2+m}$ [8] (SALT-20)	0.85	1.6 (675 K)
		$(Pb_{0.95}Sn_{0.05}Te)_{0.92}(PbS)_{0.08}$ [9]	0.4	1.5 (650 K)

1. Venkatasubramanian, Rama, et al. Nature 413.6856 (2001): 597-602.
2. Caylor, J. C., et al. Applied physics letters 87.2 (2005): 023105.
3. Broido, D. A., and N. Mingo. Physical Review B 74.19 (2006): 195325.
4. Dresselhaus, Mildred S., et al. Advanced Materials 19.8 (2007): 1043-1053.
5. Boukai, Akram I., et al. *Nature* 451.7175 (2008): 168-171.
6. DrHarman, T. C., et al. Science 297.5590 (2002): 2229-2232.
7. Hsu, Kuei Fang, et al. Science 303.5659 (2004): 818-821.
8. Poudeu, Pierre FP, et al. Angewandte Chemie 118.23 (2006): 3919-3923.
9. Androulakis, John, et al. Journal of the American Chemical Society 129.31 (2007): 9780-9788.

Engineering & Technology
Old Dominion University: www.eng.odu.edu
Applied Research Center
Old Dominion University

Case Study of thermoelectric Atomic Layer Deposition (ALD) Nanolaminates of Bi_2Te_3/ Sb_2Te_3

Structure of Sb_2Te_3 / Bi_2Te_2 Thermoelectric Films

- Sb_2Te_3 and Bi_2Te_2 are layered chalcogenides with a weak van der Waals-like bonding along their c-axis.
- Five layers stacked along c in the sequence Te-Bi-Te-Bi-Te
- Both metal tellurides are Te initiated and Te terminated
- Te surface lack dangling bonds
- The structure cleaves across the c-axis

Compounds	Space Group	Band gap	Lattice Parameter	
			a(Å)	c (Å)
Sb_2Te_3	R-3m	0.28	4.275	30.490
Bi_2Te_3	R-3m	0.2	4.3835	30.360

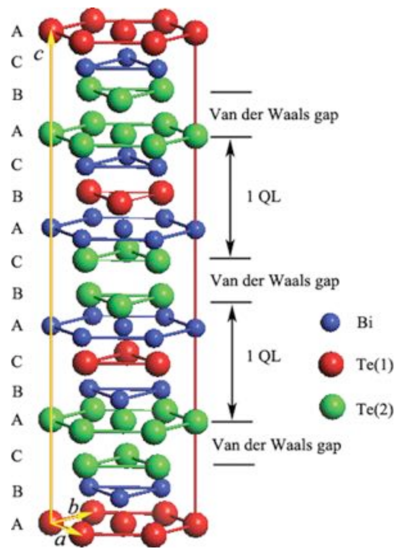

Teweldebrhan, 2010

ALD-Sb_2Te_3 / Bi_2Te_3 Multilayer Thermoelectric Films

ALD Precursors:	Deposition Temperature	Synthesized ALD Film	ALD Growth Rate
$SbCl_3 + (Me_3Si)_2Te$	70°C	Sb_2Te_3	1.2 Å/ALD cycle
$BiCl_3 + (Me_3Si)_2Te$	165°C	Bi_2Te_3	0.1 Å/ALD cycle

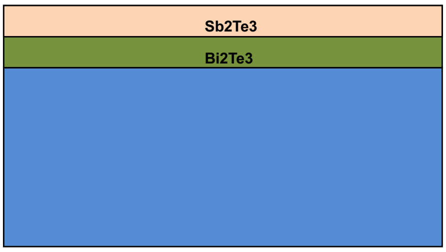

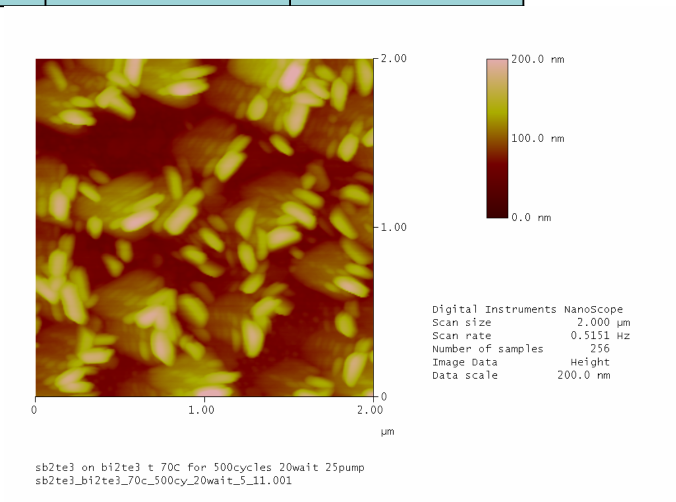

AFM micrograph revealing hexagonal platelets of ALD Sb_2Te_3 crystallites grown on a Bi_2Te_3 layer.

Trimethylsilyl telluride ($(Me_3Si)_2Te$), bismuth trichloride ($BiCl_3$) and antimony trichloride ($SbCl_3$) were utilized as chemical ALD precursors for telluride, bismuth and antimony, respectively.

Frank Batten College of
Engineering & Technology
Old Dominion University: www.eng.odu.edu

Applied Research Center
Old Dominion University

Influence of Substrate Interface Preparation on the Morphology of ALD Sb_2Te_3 Films

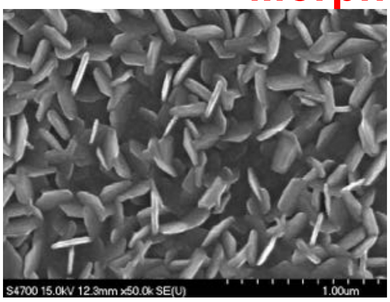

ALD Sb_2Te_3 Films grown on dry native oxide

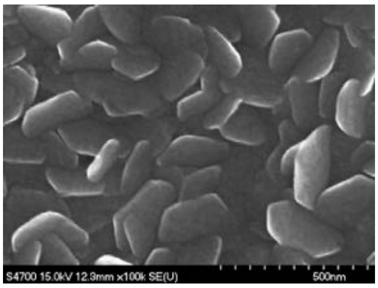

ALD Sb_2Te_3 Films grown on dry native oxide

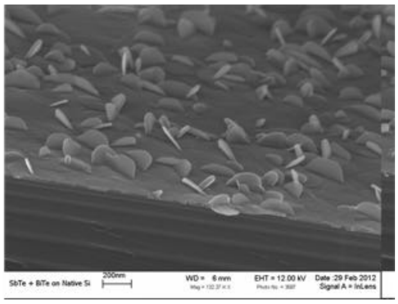

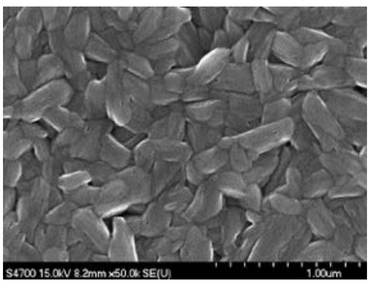

ALD Sb_2Te_3 Films grown on Platinum Interface

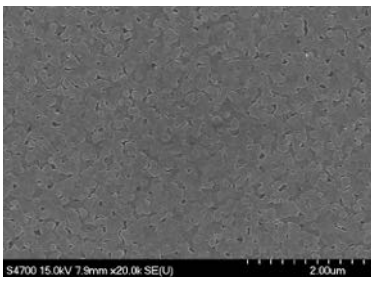

ALD Sb_2Te_3 Films grown on wet native oxide with OH^- hydroxyl surface termination.

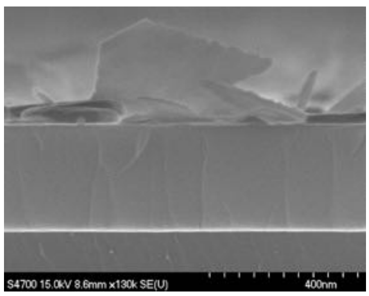

The role of OH^- termination (hydroxyl groups) of SiO_2 interfaces and Dry oxides versus wet oxides

Frank Batten College of
Engineering & Technology
Old Dominion University: www.eng.odu.edu

Applied Research Center
Old Dominion University

Influence of Deposition Temperature on The Resulting Morphology & Quality of ALD Sb_2Te_3 Films

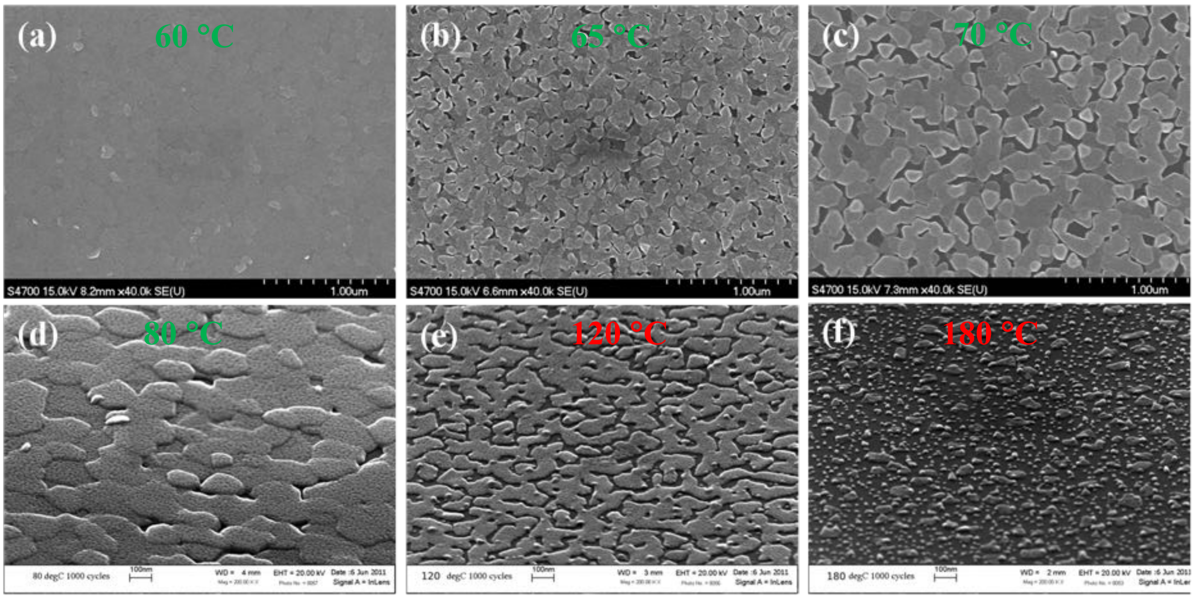

These ALD Sb_2Te_3 films (1000 ALD cycles) were grown on wet oxide with OH^- hydroxyl surface groups.

TEM cross-sectional Analysis of ALD Laminate of Bi_2Te_3 and Sb_2Te_3 Films (FEI Titan80-300)

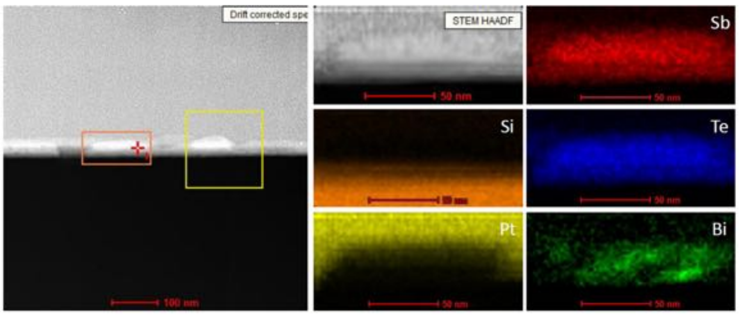

Energy dispersive X-ray spectroscopy (EDS) analysis identifying the constituents Sb, Bi and Te of the ALD films

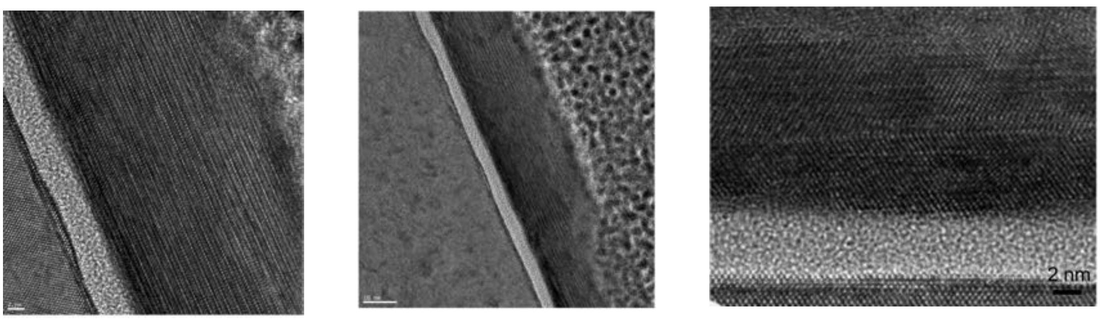

ALD Bi_2Te_3 Nanolaminate structure of alternating and Sb_2Te_3 layers exhibiting localized epitaxial growth as revealed by high resolution TEM X-section analysis. The alternating telluride films grow localized in graphene like fashion in hexagonal layers.

Frank Batten College of Engineering & Technology
Old Dominion University: www.eng.odu.edu

Applied Research Center
Old Dominion University

Growth Mechanism of ALD Films of Sb_2Te_3

Three basic growth mechanisms for thin film growth:

- **Volmer – Weber (Island growth)**
- **Frank Van der Merve (Layer by Layer growth)**
- **Stranski-Krastanov (Layer-by-Layer growth followed by island growth)**

Our experimental data identify **Volmer-Weber Island Growth** as the growth mechanism for ALD Films of Sb_2Te_3.

Volmer-Weber Growth

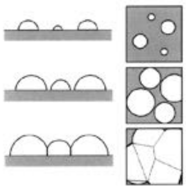

- This type of growth is favorable when the adatom-adatom interaction is more significant than the interaction of adatom with the surface
- The layers grow as islands centered on the nucleating sites
- These islands further grow to impinge and coalesce forming continuous film

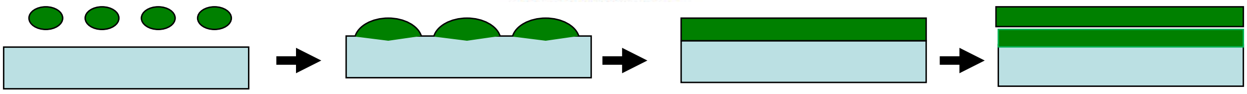

Case Study thermoelectric ALD Nanolaminates of PbTe/ PbSe Films

Frank Batten College of
Engineering & Technology
Old Dominion University: www.eng.odu.edu

Applied Research Center
Old Dominion University

▪ Physical Properties of PbTe and PbSe

- PbTe and PbSe work in intermediate temperature range up to 850 K, which is the sweet spot for thermoelectric use.
- PbTe and PbSe are narrow band lead chalcogenides with FCC rock salt structure.
- PbTe and PbSe have low thermal conductivity and good electrical conductivity.

ZT

Material	Bandgap	Thermal conductivity	Hole Mobility	Electron mobility	Lattice constant	Melting point
PbTe	0.25 eV	2.30 W/mK	600 cm^2/Vs	1600 cm^2/Vs	6.438 Å	907°C
PbSe	0.26 eV	1.70 W/mK	900 cm^2/Vs	1000 cm^2/Vs	6.1243 Å	1067°C

ALD Process for the Synthesis of PbTe & PbSe

$$Pb(C_{11}H_{19}O_2)_2\ (g) + (Me_3Si)_2Te\ (g) \Longrightarrow PbTe\ (s) + 2Me_3SiC_{11}H_{19}O_2(g)$$

lead(II)bis(2,2,6,6-tetramethyl-3,5-heptanedionato)

(trimethylsilyl)telluride

$$Pb(C_{11}H_{19}O_2)_2\ (g) + (Et_3Si)_2Se\ (g) \Longrightarrow PbSe\ (s) + 2Et_3SiC_{11}H_{19}O_2(g)$$

(triethylsilyl)selane

❑ PbTe, PbSe films were grown by ALD on silicon substrates using $Pb(C_{11}H_{19}O_2)_2$, lead(II)bis(2,2,6,6-tetramethyl3,5-heptanedionato) as the lead precursor, and $(Me_3Si)_2Te$, (trimethylsilyl)telluride as the tellurium precursor, and $(Et_3Si)_2Se$ (triethyl silyl)selane as the selenium precursors.

❑The lead precursor was heated to 140° C, the telluride precursor to 40° C and the selenium precursor remained at room temperature.

❑ Nitrogen N_2 gas was used as a carrier for the precursors. The ALD base chamber pressure was 40 mTorr.

Frank Batten College of
Engineering & Technology
Old Dominion University: www.eng.odu.edu
Applied Research Center
Old Dominion University

Results and Discussions

- **TEM Cross-sectional Micrographs of ALD PbTe Films**

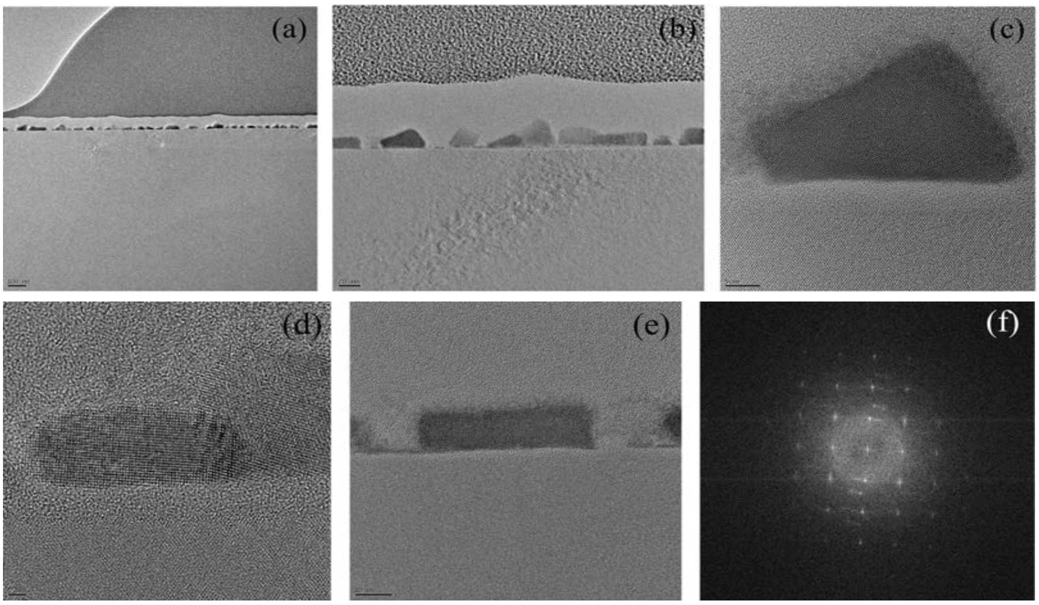

(a) and (b) Transmission Electron Microscopy (TEM) cross-sectional analysis of ALD deposited PbTe films; (c) low magnification overview of ALD deposited films, (d) and (e) high resolution microstructure of individual PbTe crystallites; and (f) TEM selective area diffraction pattern.

- The TEM data is in agreement with XRD, which confirms the presence of poly crystalline PbTe.
- The measured lattice constant of 6.440 nm closely matches with the reference value of crystalline PbTe .

Zhang, K., et al. *ECS Journal of Solid State Science and Technology* 3.6 (2014): P207-P212.

TEM Crosssection Micrographs of ALD PbTe Films

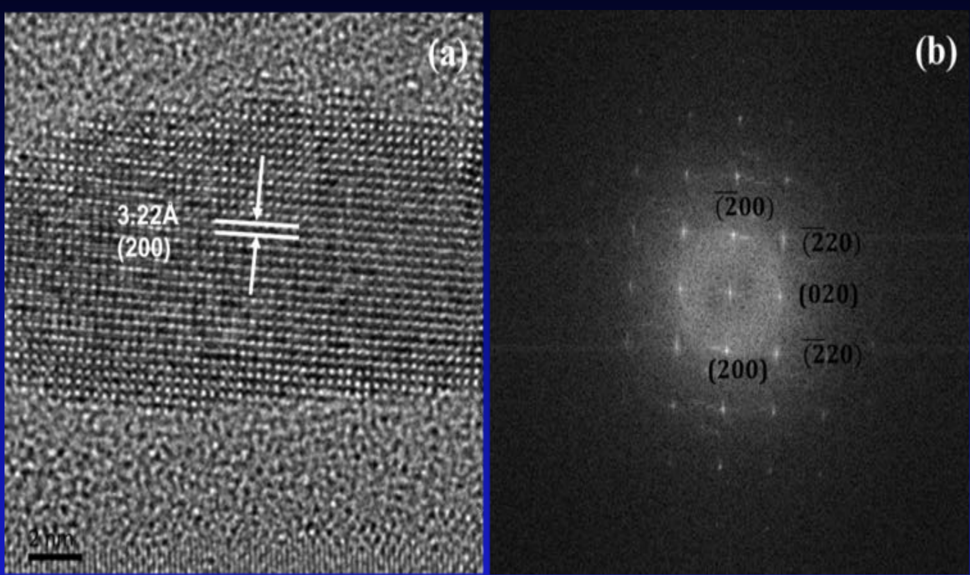

Transmission Electron Microscopy (TEM) cross-sectional analysis of ALD deposited PbTe films (a) high resolution microstructure of individual PbTe crystallites, and (b) a fast Fourier transform pattern.

- The TEM data is in agreement with XRD, which confirms the presence of poly crystalline PbTe.
- The measured lattice constant of 6.440 nm closely matches with the reference value of crystalline PbTe .

Structure of ALD PbTe-PbSe Nanolaminate Films

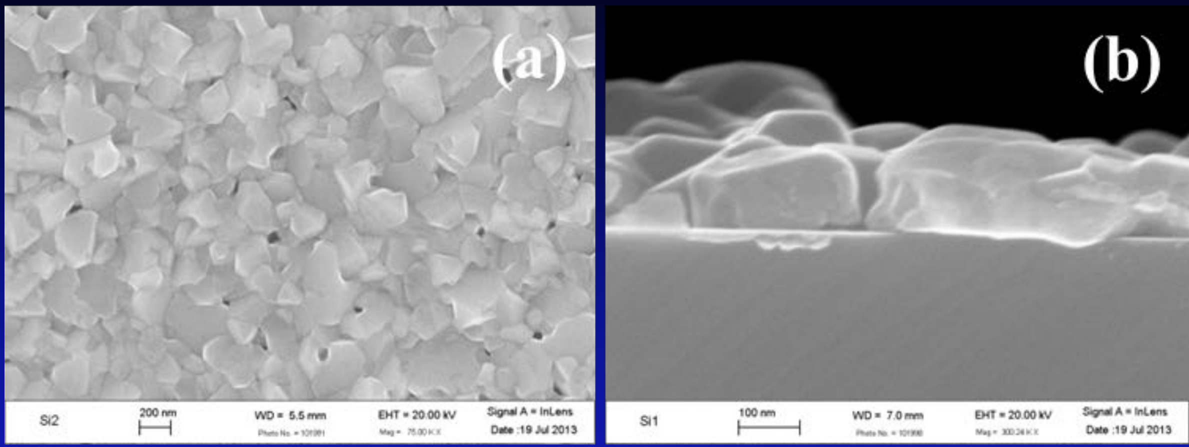

FE-SEM images of basic PbTe-PbSe film structure consisting of 5000 ALD cycles (PbTe) plus 4000 cycles (PbSe) on top of it which may be optimized further into nanolaminate structures (a) planar view and (b) cross-sectional view.

- **Initially, heterogeneous nucleation sites form and with more ALD cycles the grains grow horizontally and vertically into larger islands.**
- **The initial rock salt structure disappears as islands conglomerate with increased ALD cycles to provide full surface coverage.**

Zhang, K., et al. *ECS Journal of Solid State Science and Technology* 3.6 (2014): P207-P212

Results and Discussions

❖ Surface Characterization

- **FE-SEM Micrographs Displaying Surface Morphology of ALD Synthesized PbSe, PbTe Films and PbTe/PbSe Nanolaminates on Si Substrates**

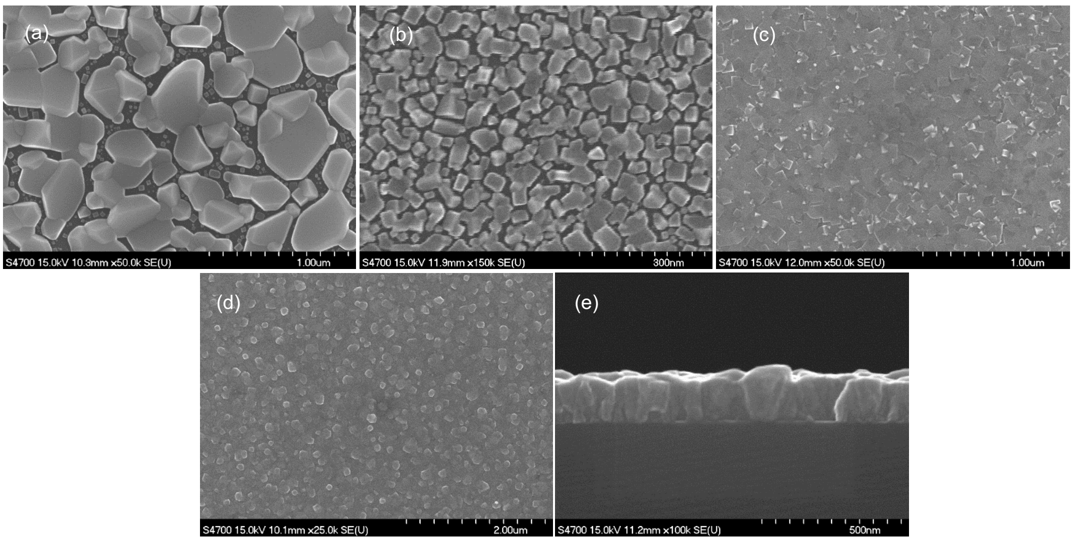

FE-SEM images of (a) 1000 ALD deposition cycles of PbTe films without hydroxyl OH^- treatment, (b) 1000 ALD cycles of PbSe films without hydroxyl OH^- treatment, (c) 1000 ALD cycles of PbSe film with hydroxyl OH^- treatment, (d) PbTe/PbSe (10/10 nm) nanolaminates, (e) Cross-section micrograph of PbTe/PbSe (10nm/10 nm) nanolaminate films.

Frank Batten College of
Engineering & Technology
Old Dominion University: www.eng.odu.edu
Applied Research Center
Old Dominion University

Results and Discussions

- **X-ray Diffraction (XRD) Analysis of ALD PbTe Film, PbSe Film and Double Layer PbTe/PbSe Film**

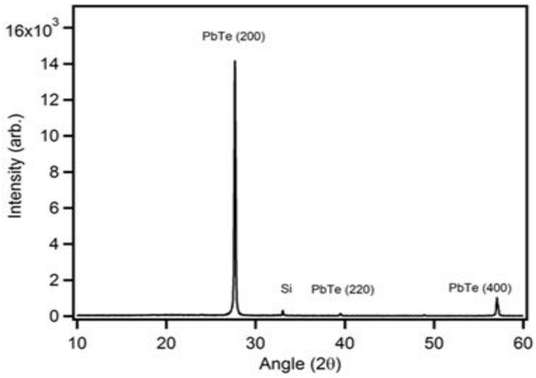

XRD for PbTe (170 ˚C, 2000 cycles)

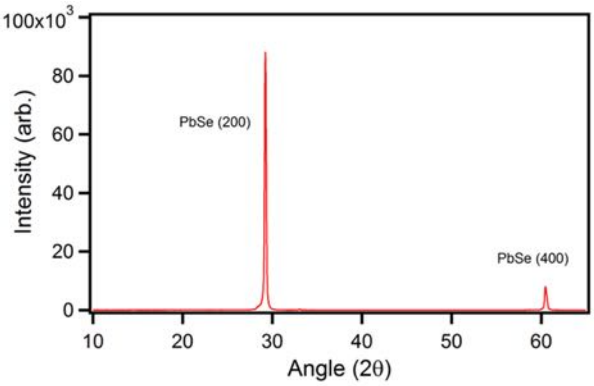

XRD for PbSe (170 ˚C, 4000 cycles)

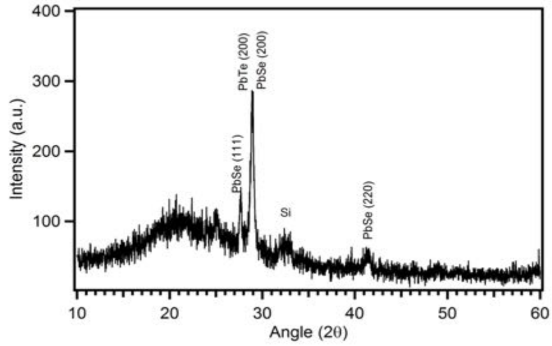

XRD for 5000 cycles PbTe and 4000 cycles PbSe (170 ˚C)

Zhang, K., et al. *ECS Journal of Solid State Science and Technology* 3.6 (2014): P207-P212.

Results and Discussions

- **AFM Images of Triple Layer ALD PbTe/PbSe/PbTe Film**

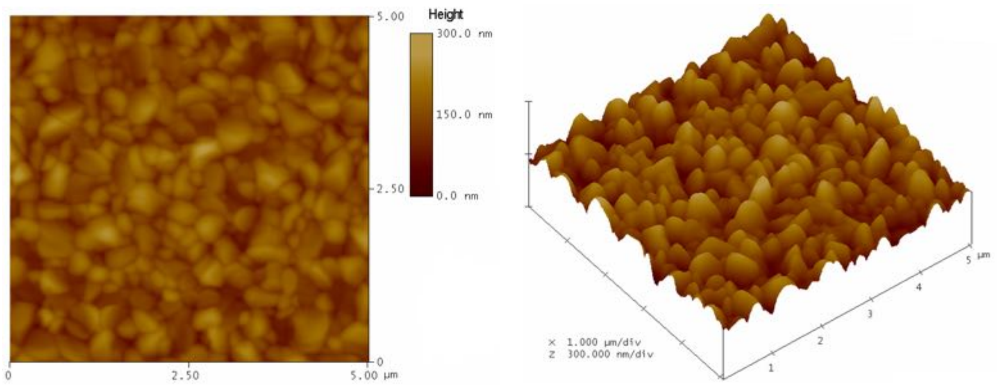

Triple layers of PbTe / PbSe / PbTe (using 5000 / 4000 / 6000 ALD deposition cycles) was deposited on Si substrate at 170 ˚C. The film thickness is around 355 nm. The roughness of the film is about 31.79 nm.

Basic Building Block of an ALD PbTe/PbSe double Layer Nanolaminate Structure on flat planar Si Substrates

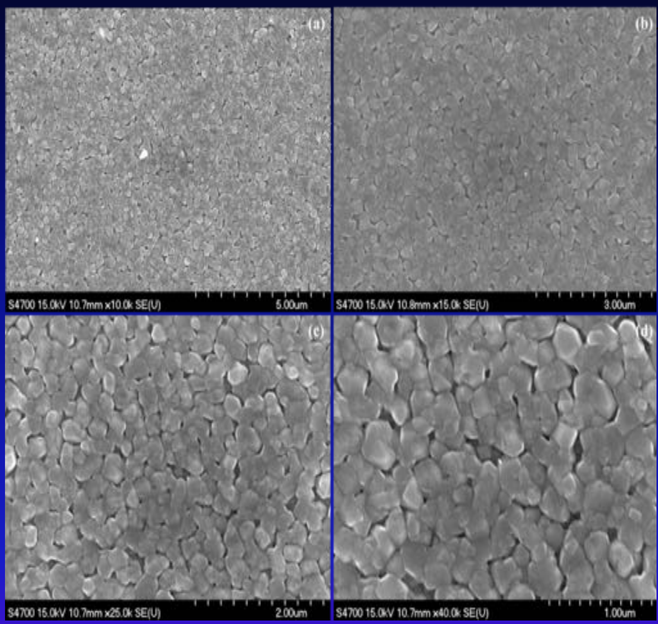

• FE-SEM images of PbTe-PbSe film morphology for double layer consisting of 10150 ALD deposition cycles of (PbTe) plus 11400 ALD cycles of (PbSe) on top of it deposited at 170 ^{o}C.

High Angle Annular Dark Field STEM and EDX Spectra and Mapping Results

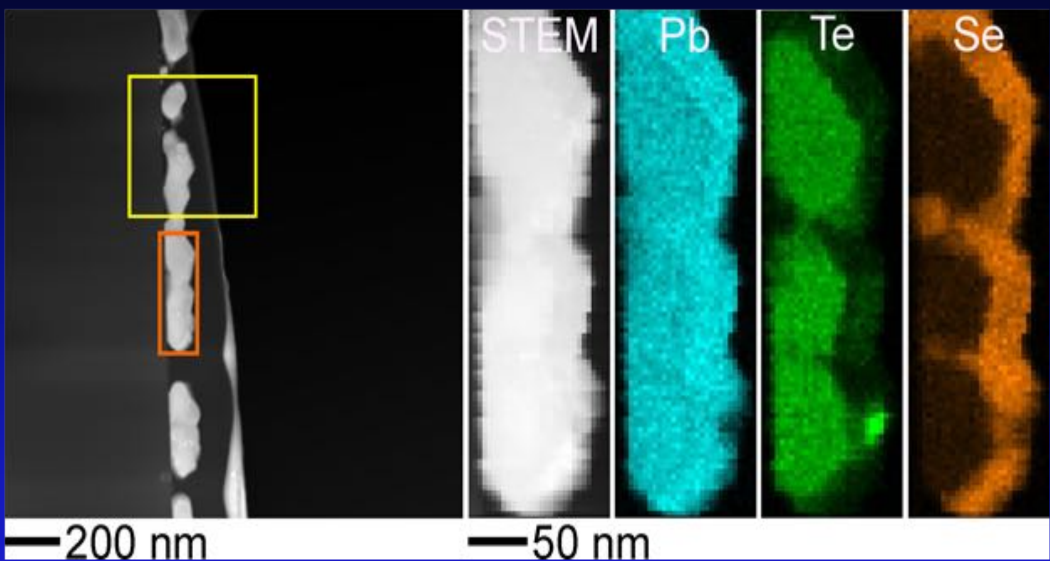

❑ HAADF-STEM image and the corresponding EDS elemental maps of Pb, Se and Te from the PbTe/PbSe clearly delineate the two distinct layers of a basic nanolaminate composite with ALD PbSe on top of ALD PbTe. The orange window marks the area mapped and the yellow window represents the drift correction are used.

Proposed Solution: Thermoelectric ALD Nanolaminate Film Coatings inside Porous Templates

- **Fabricate thermoelectric materials (PbSe, PbTe and PbSe/PbTe superlattices) using conformal coatings of high aspect ratio structures to minimize cost and to allow the formation of relatively thick layers of > 200nm by depositing just few 100nm superlattice structures in periodic Porous Templates.**

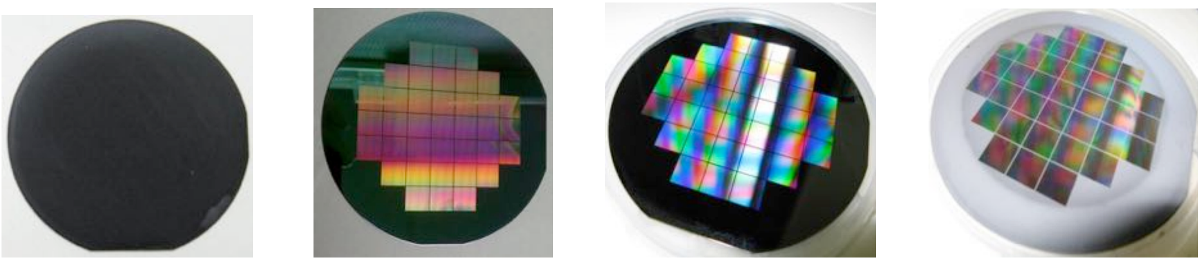

- Si wafer Photolithography RIE/KOH etching Post-treatment

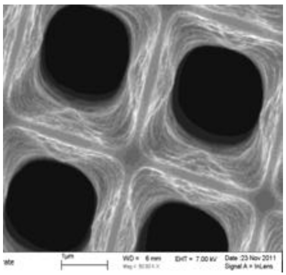

Conformal coatings of ALD PbTe & PbSe film depositions were evaluated

Motivation

✓ **Nano-patterning of thermoelectrical materials for Phonon-scattering Engineering**

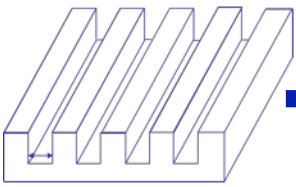

Patterning into stripes for subsequent ALD deposition of PbSe layers with different thickness

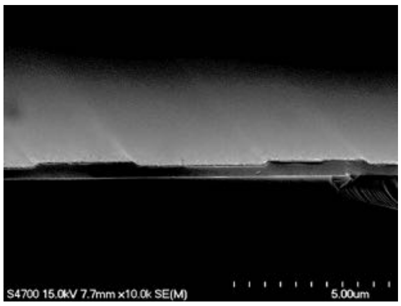

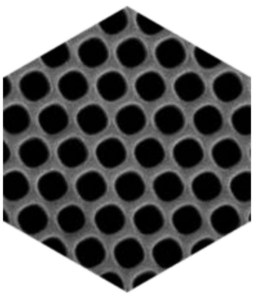

Patterning into porous membranes for subsequent ALD deposition of PbTe/PbSe nanolaminates with different periods

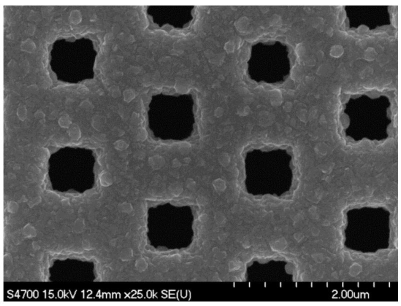

Frank Batten College of
Engineering & Technology
Old Dominion University: www.eng.odu.edu
Applied Research Center
Old Dominion University

Micropore Templates are defined with Mask & Photolithography

Top

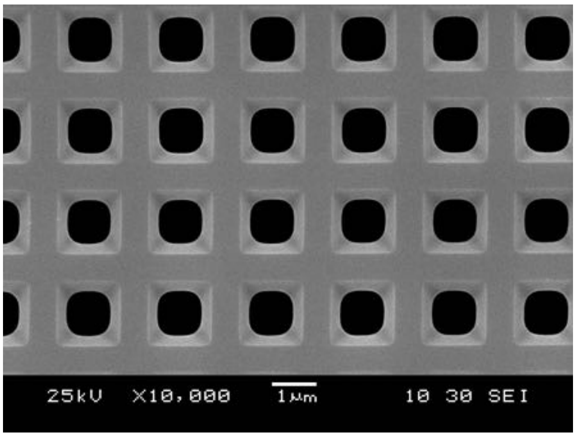

Bottom

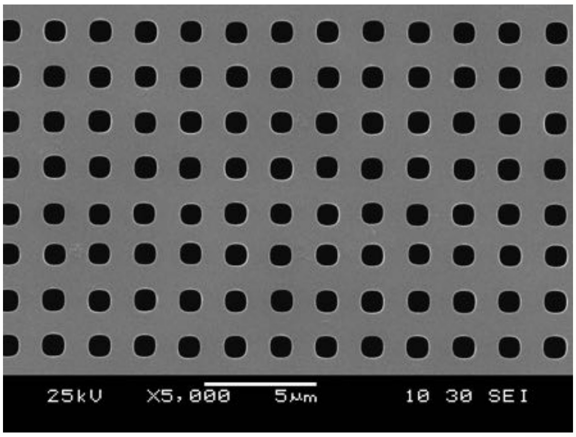

Results and Discussions of Porous Templates

- **FE-SEM Micrographs of ALD PbSe/PbTe Film Coatings inside the Pore Walls of Porous Si Templates**

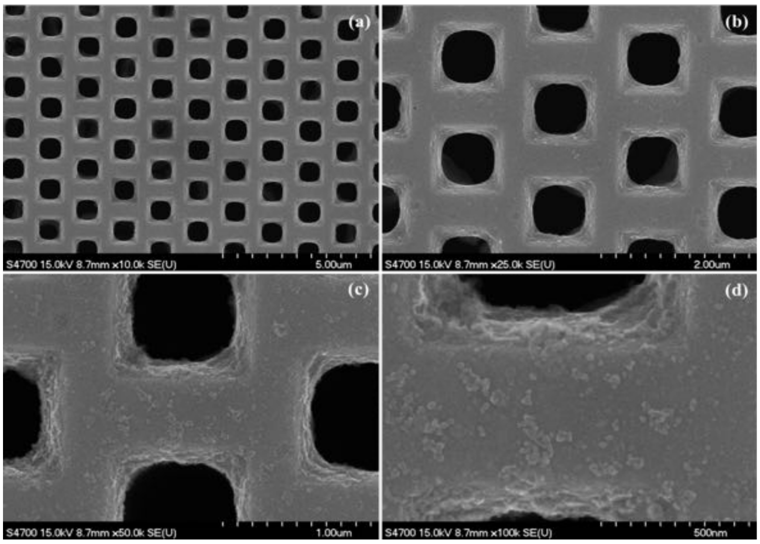

Total 6 alternating layers of PbTe / PbSe (1000 / 1000 ALD cycles) nanolaminates was deposited on porous Si substrates by ALD, grown at 170 ˚C. The film thickness is around 270 nm.

Results and Discussions of Porous Templates

❖ Surface Characterization

- **FE-SEM Micrographs Displaying Surface Morphology of ALD Synthesized PbSe/PbTe Nanolaminates inside Porous Si Templates**

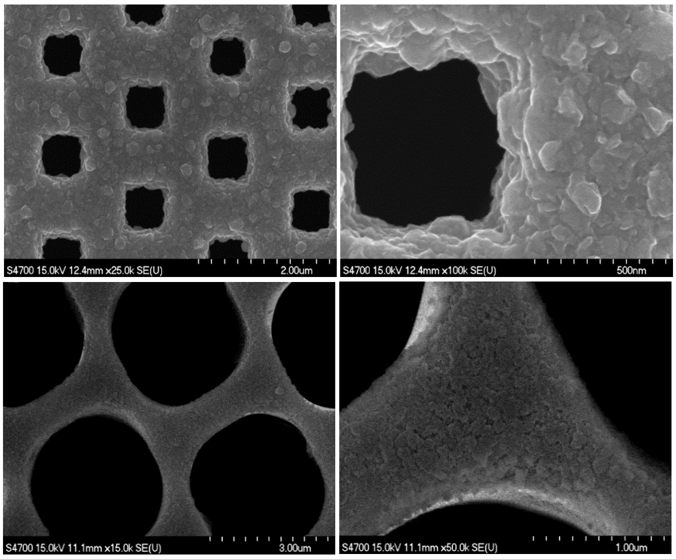

PbTe / PbSe (10 nm / 10 nm) ALD nanolaminate coatings were deposited on porous Si substrates by ALD at 150 ˚C. The film thickness is around 170 nm. The top two SEM micrographs reveal misaligned square pores of 700 nm size, while the two bottom micrographs show misaligned round square pores with pore size of 3 µm and a pore wall width of 600 nm.

Electrical Seebeck Measurements of Nanostructured ALD Nanolaminate Films of PbTe/ PbSe on Nanoporous Si Substrates benchmarked against ALD thermoelectric Films on Planar Si Substrates

Seebeck Results on Planar Si Substrates

- **Seebeck Measurement of Double Layered ALD PbTe / PbSe Film**

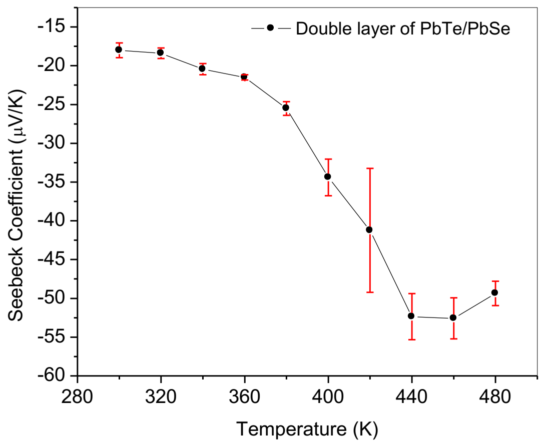

Seebeck measurement of double layered PbTe/PbSe sample

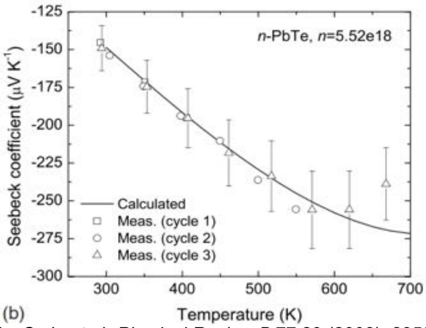

Vineis, C. J., et al. *Physical Review B* 77.23 (2008): 235202.

- ❑ Double layered PbTe/PbSe (10150 / 10400 cycles) samples were measured by MMR Seebeck Measurement System.
- ❑ The Seebeck coefficient in horizontal direction was measured from 300K to 480 K in 20 K interval steps.
- ❑ The negative Seebeck readings across temperature indicate that the sample is n-type material.
- ❑ The Seebeck coefficient increases as temperature is increasing, and reaches a maximum value at 460 K, and then decreases as the temperature is further increasing.

Seebeck Results on Planar Si Substrates

- **Seebeck Measurement of Triple layer ALD Synthesized PbTe/PbSe/PbTe Samples**

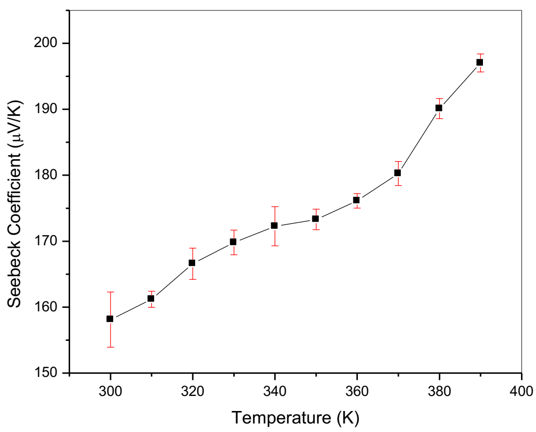

Triple layered ALD PbTe / PbSe / PbTe sample

- ❑ Triple layered PbTe/PbSe/PbTe samples were measured by MMR Seebeck Measurement System.
- ❑ The Seebeck coefficient in horizontal direction was measured from 300K to 390 K in 10K steps.
- ❑ The Seebeck readings as a function of temperature indicate that the material is a p-type.

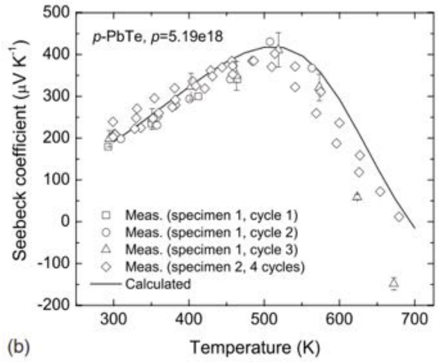

Vineis, C. J., et al. *Physical Review B* 77.23 (2008): 235202.

Electrical Seebeck Results of Thermoelectric Film Coatings on Nanoporous Si Templates

❖ Seebeck Coefficient Measurement

- **Seebeck Measurements of ALD PbTe / PbSe Nanolaminates Synthesized on Silicon and inside of Porous Si Templates**

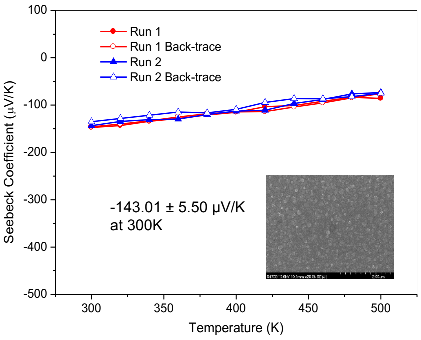

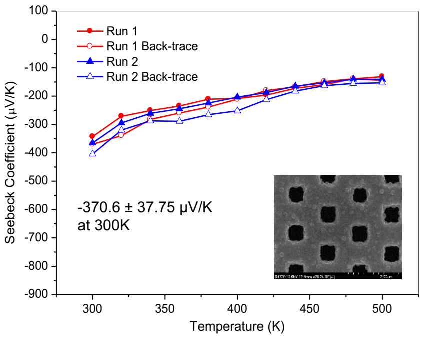

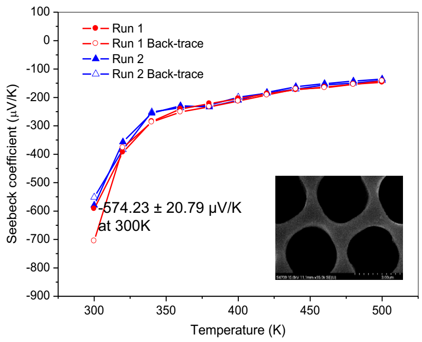

ECS Journal of Solid State Science and Technology, 5(9) 503-508, (2016)

Seebeck coefficient of PbTe/PbSe (10 nm/ 10 nm) nanolaminates deposited on (a) Planar Si wafer and (b) microporous Si templates with square pore size of 700 nm and the width of pore wall of 700 nm (c) microporous Si templates with pore size of 3 um and the width of pore wall of 600 nm over the temperature range of 300 K～500 K in in-plane direction by MMR Seebeck Measurement System. The negative value of Seebeck coefficient indicates the sample is n-type, and charged carriers are electrons.

Frank Batten College of Engineering & Technology
Old Dominion University: www.eng.odu.edu

Applied Research Center
Old Dominion University

Electrical Seebeck Results of Thermoelectric Film Coatings on Porous Si Templates

The Enhanced Seebeck coefficient of the porous nanolaminates results from the lower thermal conductivity in the porous samples using the advantageous staggered square pore configuration.

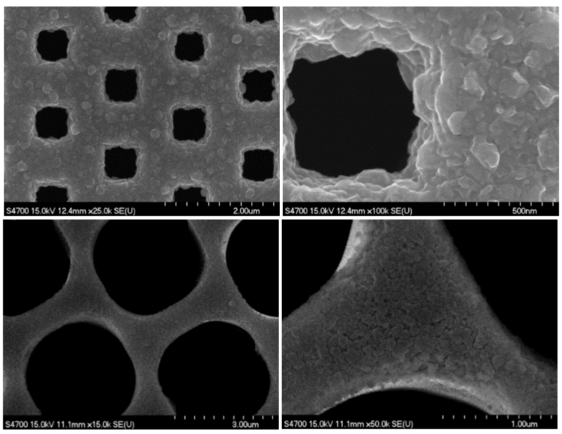

PbTe / PbSe (10 / 10 nm) nanolaminates was deposited on porous Si substrate by ALD

X. Chen, et al. Journal of Solid State Science and Technology, 5(9) 503-508, (2016)

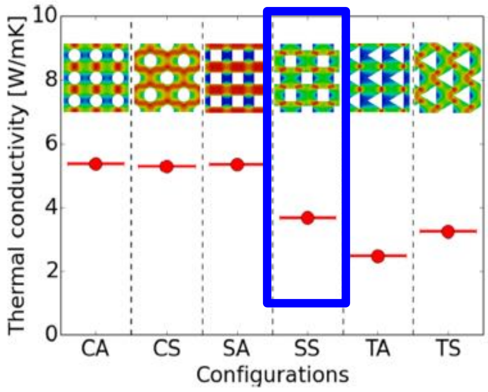

Phonon thermal conductivity for different configurations. APL. **105**,033116 (2014).

$$S = -\frac{\Delta V}{\Delta T}$$

Frank Batten College of Engineering & Technology
Old Dominion University: www.eng.odu.edu

Applied Research Center
Old Dominion University

Thermal Conductivity Results of Thermoelectric Film Coatings on Porous Si Templates

❖ Thermal Conductivity Measurement

- PbTe/PbSe nanolaminates with 20 cycles, 60 cycles and 100 cycles per layer, where the corresponding thickness per layer is around 2 nm, 6 nm, and 10 nm.
- The PbTe/PbSe nanolaminates grown on porous silicon exhibit much smaller thermal conductivity around 0.8 $Wm^{-1}K^{-1}$.

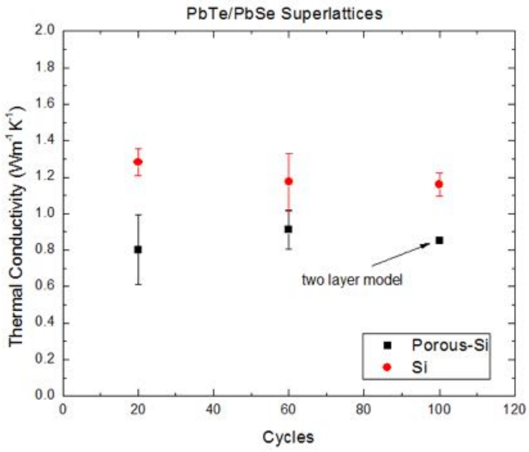

Thermal conductivity of thermoelectric Nanolaminates with different periods grown on Si wafer and porous silicon template

*Collaboration with Prof. P. Hopkins at UVA Charlottesville, Virginia.

Thermal Conductivity Results of Thermoelectric Film Coatings on Porous Si Templates

❖ Thermal Conductivity Simulation

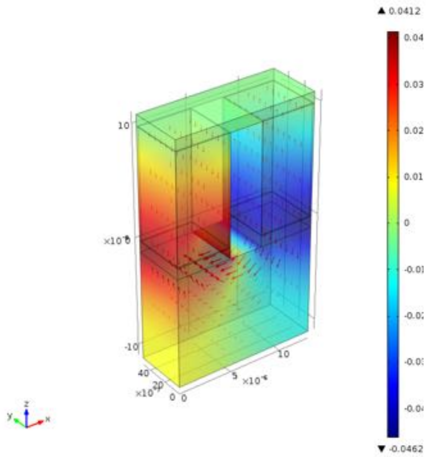

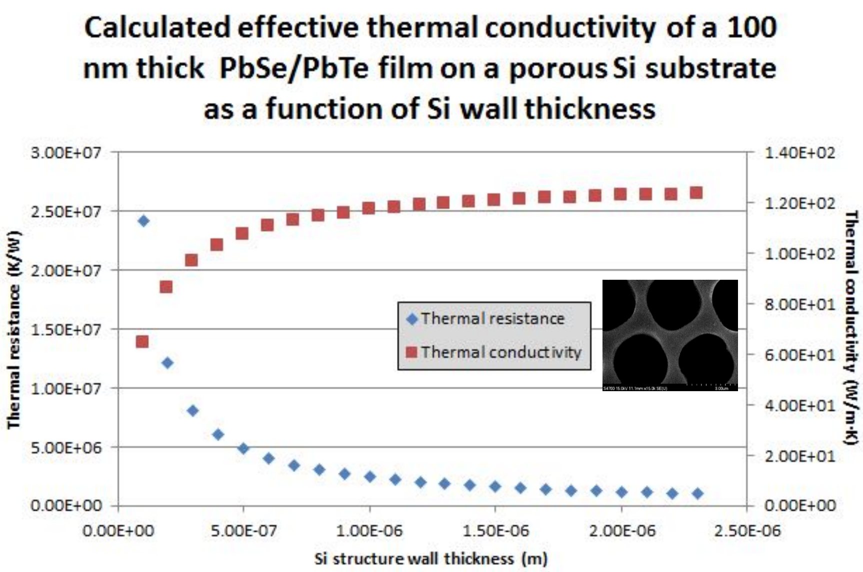

The model displaying pore walls sandwiched in copper mounted to a heatsink with a resulting effective thermal conductivity as low as 65 W/m·K.

Geist, Brian L.,… Chen, X., et al. *MRS Proceedings*. Vol. 1735. Cambridge University Press, 2015.

Nano-patterning of Thermoelectrical Materials into Stripes

❖ Fabrication of nano-patterned stripes by photolithography in Si substrates

- The stripe patterned silicon substrates with stripe width of 4 μm, 2 μm and 1 μm were fabricated by etching thermal oxidized silicon wafers in KOH solution after photolithography patterning with a stripe mask.
- The substrate were pre-treated by ultra-sonic cleaning in acetone, rinsing with DI water, and drying with nitrogen gas flow.
- The pre-treated substrates were put in furnace in convection with N_2 gas flow at 120 ˚C for 15 min to dehydrate before applying HMDS as surface promotor.
- The Mir-701 photoresist was spin-coated with spin speed of 4000 rpm resulting in ~ 0.9 μm thick film.
- The sample coated with photoresist was soft baked on hot plate at 90 ˚C for 1 min.
- The sample was exposed under UV light with intensity of 2.55 mW/cm^2 for 1 min in hard contact mode.
- After 1 min Post Exposure Bake at 110 ˚C , the exposed sample was developed in diluted MIF 300 developer for 65 sec.
- The sample was then post backed in hot plate at 100 ˚C for 10 min, and then etched in BOE solutions for 10 min.
- The sample was then etched in diluted KOH solution. The remaining photoresist will be removed by diluted KOH solution in 1 min, therefore there are still patterned silicon dioxide layer left acting as isolated layer.

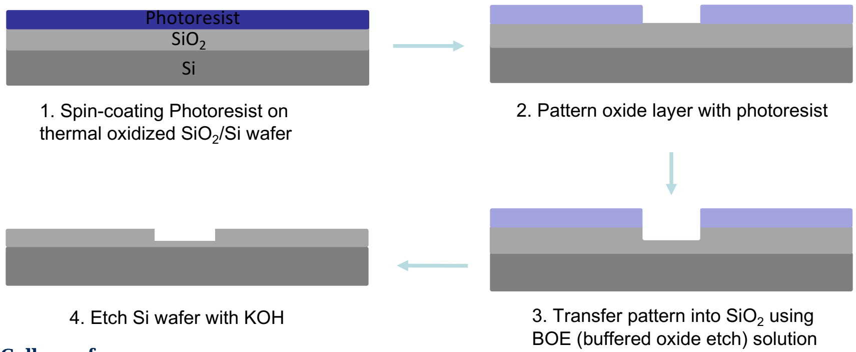

Frank Batten College of Engineering & Technology
Old Dominion University: www.eng.odu.edu

Applied Research Center
Old Dominion University

Nano-patterning of Thermoelectrical Materials into Stripes

❖ Surface Characterization

- **FE-SEM Micrographs Displaying Surface Morphology of ALD Synthesized PbSe on Stripe patterned Si Substrates**

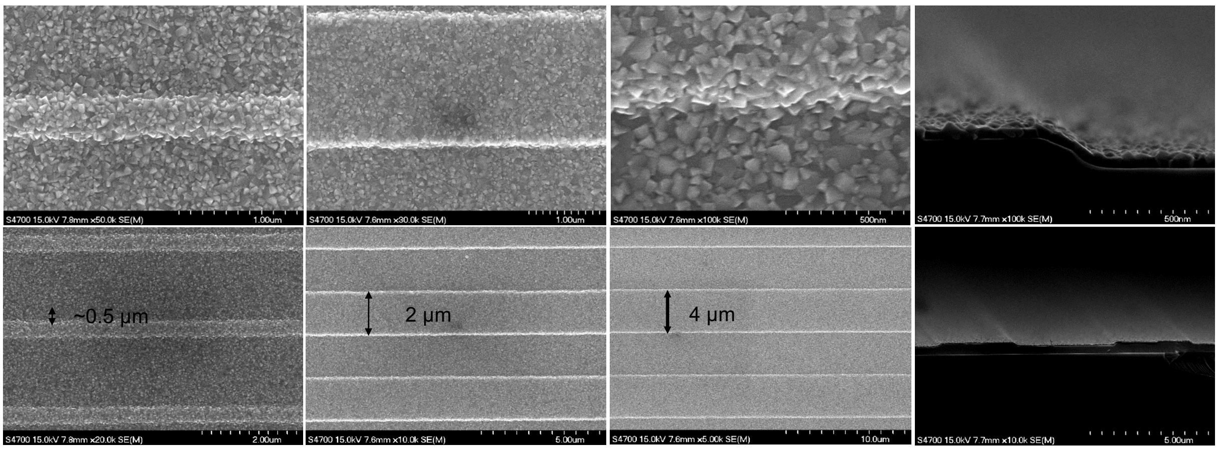

(a) (b) (c) (d)

FE-SEM images PbSe film on (a) 0.5 - 1μm, (b) 2 μm, (c) 4 μm patterned Si substrate, (d) cross-sectional images of PbSe film grown on 2 μm wide stripe patterned Si substrate

Frank Batten College of Engineering & Technology
Old Dominion University: www.eng.odu.edu

Applied Research Center
Old Dominion University

Seebeck Results of Nano-patterned Stripes of Thermoelectrical Materials

❖ Seebeck Coefficient Measurement

- **Seebeck Measurements of ALD PbSe Synthesized on Stripe patterned Silicon**

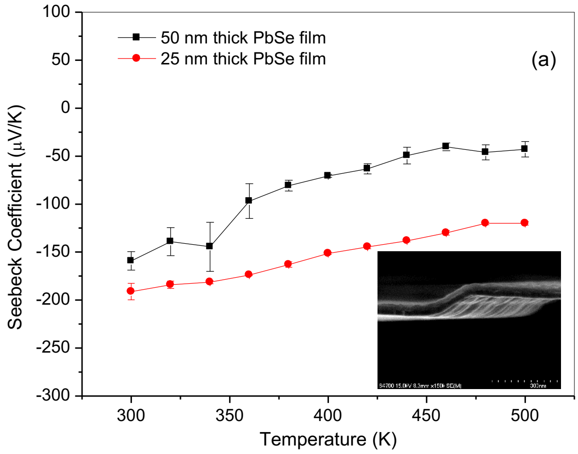

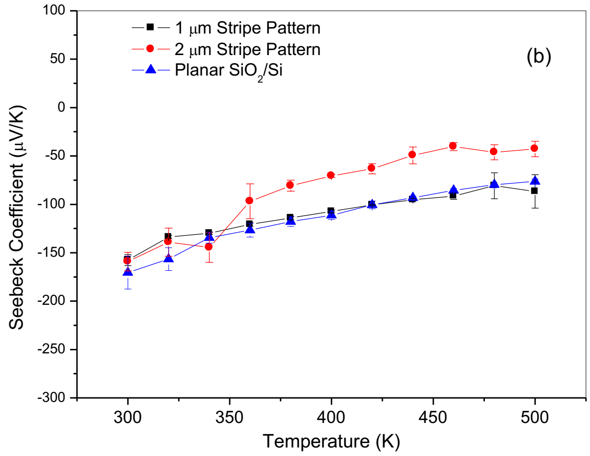

(a) Seebeck coefficient of PbSe film with thickness of 50 nm and 25 nm grown on 2 μm wide stripe patterned Si substrate over a temperature range of 300 K ~ 500 K. (b) Seebeck coefficient of PbSe films with thickness of 50 nm grown on stripe patterned Si substrate with width of 1 μm and 2 μm and planar SiO_2/Si wafer over temperature range of 300 K ~ 500 K in in-plane direction by MMR Seebeck Measurement System. The negative value of Seebeck coefficient indicates the sample is n-type, and charged carriers are electrons.

Outlook on new Materials:

Seebeck Coefficient Measurements of Polycrystalline and Highly Ordered Surface Anchored Metal-Organic Framework (SURMOF) Thin Films

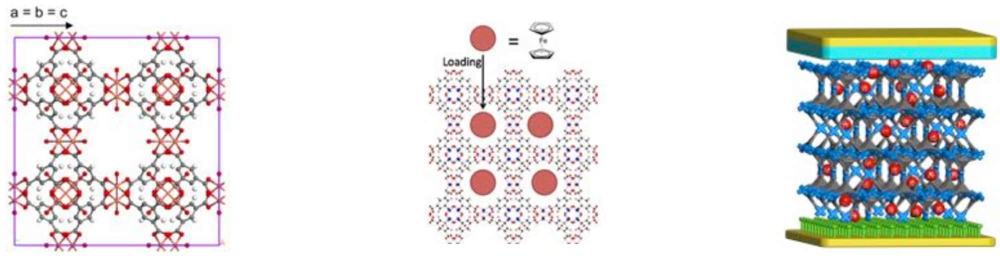

Structure/architecture of the porous solids used in the present study. (a) HKUST-1 with a=26.343Å. (b) HKUST-1 unit cell loaded with Ferrocene.

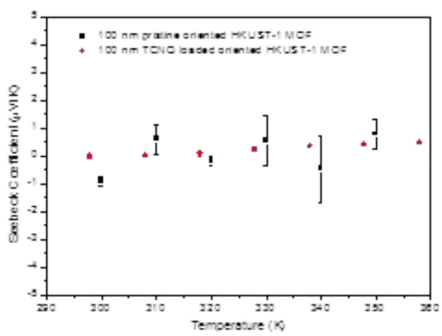

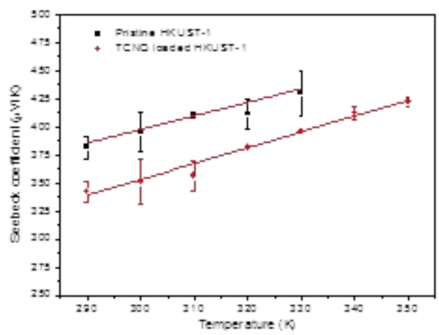

(a) Seebeck coefficient measurements as function of temperature of LPE highly oriented HKUST-1 films with a thickness of 100 nm, which were prepared with and without TCNQ loading. (b) Seebeck coefficient measurements of LPE polycrystalline HKUST-1 thin film with a thickness of 200 nm, which were prepared with and without TCNQ loading.

Frank Batten College of Engineering & Technology
Old Dominion University: www.eng.odu.edu

Applied Research Center
Old Dominion University

Conclusions

- ALD PbSe films were deposited on stripe patterned Si substrates with width of 1 μm, 2μm and 4 μm. Al_2O_3 layer with thickness of 20 nm was coated as protection layer. ALD PbTe/PbSe based nanolaminates (NL) Thermoelectric materials were successfully synthesized on planar silicon wafers and inside porous silicon templates.
- The width of stripe pattern has a measurable influence on the Seebeck coefficient of PbSe film in horizontal in-plane direction at high temperature. The reduction of film thickness also reveals an improvement of the Seebeck coefficient of PbSe film.
- ALD PbTe/PbSe Nanolaminates synthesized inside periodic porous silicon templates exhibit significant higher Seebeck coefficients of 574.239 μV/K in horizontal in-plane direction compared to planar Si substrates.
- The thermal conductivity results of ALD PbTe/PbSe Nanolaminate structures indicate the porous templates contribute to a significant reduction of the thermal conductivity of the ALD Nanolaminate structure.
- The ALD Nanolaminates with lower thickness per layer exhibits lower thermal conductivity. The PbTe/PbSe Nanolaminates with 20 ALD cycles per layer grown on porous silicon template exhibit lowest thermal conductivity about 0.22 W/(m·K), resulting from thinner Si pore walls and enhanced phonon scattering by larger density of interfaces from multiple islands and NL layers.
- Phonon-boundary engineering is a novel approach to reduce lattice thermal conductivity by nano-patterning ALD thermoelectric films approaching the dimensions of the phonon mean free path, and thus improve the figure of merit of Thermoelectric materials.
- A new method for obtaining high ZT thermoelectric Materials by nanostructured ALD is suggested. A path towards obtaining a higher Power Factor is outlined.
- A Novel Approach for growing low thermal conductivity Thermoelectric material by ALD is demonstrated.